

Entrance Region Flow Heat Transfer in Concentric Annuli with Rotating Inner Wall for Bingham Fluid

Srinivasa Rao Nadiminti^{1*}, Adiyapatham Kandasamy¹

RESEARCH ARTICLE

Received 05 January 2016; accepted after revision 25 February 2016

Abstract

A finite difference analysis of the entrance region flow heat transfer of Bingham fluid in concentric annuli with rotating inner wall has been carried out. The analysis is made for simultaneously developing hydrodynamic and thermal boundary layer in concentric annuli with one wall being isothermal and other one being adiabatic. The inner cylinder is assumed to be rotating with a constant angular velocity and the outer cylinder being stationary. A finite difference analysis is used to obtain the velocity distributions, pressure drop and temperature variations along the radial direction. Computational results are obtained for various values of aspect ratio N , Bingham number B and Prandtl's number. Comparison of the present results with the results available in literature for various particular cases has been done and found to be in agreement.

Keywords

concentric annuli, Bingham fluid, entrance region flow, heat transfer, finite difference method, rotating wall

1 Introduction

The study of non-Newtonian laminar flow heat transfer in thermal entrance region of an annuli is of practical importance in engineering applications such as design of compact heat exchangers, axial-flow turbo machinery and polymer processing industries. Very often, optimum conditions are provided by laminar flow operations for keeping low pumping power in proportion to the heat transfer rate. In the nuclear reactor field, this happens when coolant flow rates are reduced. In case of turbulent flow, when heating starts at the duct entrance, the hydrodynamic boundary layers normally are linear near the duct entrance and the transitions to turbulence occurs at some distance downstream from the entrance. Hence, it is necessary to take into consideration the presence of such laminar entrance flow in calculating the heat transfer parameters for a duct in which the fully developed flow is turbulent. Many important industrial fluids are non-Newtonian in their flow characteristics and are referred to as rheological fluids. These include blood; various suspensions such as coalwater or coal-oil slurries, glues, inks, foods; polymer solutions; paints and many others. The fluid considered here is the Bingham model, which is of 'time-independent yield stress' fluid category.

The problem of entrance region flow heat transfer in a concentric annuli for a Newtonian fluid was studied by Coney and El-Shaarawi [1]. Mishra et al. [2] studied the flow of the Bingham plastic fluids in the concentric annulus and obtained the results for boundary layer thickness, centre core velocity, pressure drop. Batra and Bigyani Das [3] developed the stress-strain relation for the Casson fluid in the annular space between two coaxial rotating cylinders where the inner cylinder is at rest and outer cylinder rotating. Maia and Gasparetto [4] applied finite difference method for the Power-law fluid in the annuli and found difference in the entrance geometries. Sayed-Ahmed and Hazem [5] have applied finite difference method to study the laminar flow of a Power-Law fluid in a concentric annuli with rotating inner wall.

The constitutive equation for Bingham fluid is given as Bird et al. [6]

¹ Department of Mathematical and Computational Sciences, National Institute of Technology Karnataka, Surathkal, Mangalore, India-575025, India

* Corresponding author, e-mail: srinudm@gmail.com

$$\tau_{ij} = \left(\mu + \frac{\tau_0}{\varepsilon} \right) \varepsilon_{ij} \quad (\tau \geq \tau_0) \quad (1)$$

where

$$\tau = \sqrt{\frac{1}{2} \tau_{ij} \tau_{ij}} \quad \text{and} \quad \varepsilon = \sqrt{\frac{1}{2} \varepsilon_{ij} \varepsilon_{ij}}$$

here τ_0 is the yield stress, τ_{ij} and ε_{ij} are the stress tensor and the rate-of-strain tensor, respectively. and μ is the viscosity of the fluid.

Kandasamy [7] investigated the entrance region flow heat transfer in concentric annuli for a Bingham fluid and presents the velocity distributions, temperature and pressure in the entrance region. Round and Yu [8] analyzed the developing flows of Herschel-Bulkley fluids through concentric annuli. Further, entropy generation in Non-Newtonian fluids due to heat and mass transfer in the entrance region of ducts has been investigated by Galanis and Rashidi [9]. Rashidi et al. [10] analyzed the pulsatile flow through annular space bounded by outer porous cylinder and an inner cylinder of permeable material. Moreover, Rashidi et al. [11] studied the investigation of heat transfer in a porous annulus with pulsating pressure gradient by homotopy analysis method. Recently, Kandasamy and Srinivasa Rao [12, 13] investigated entrance region flow in concentric annuli with rotating inner wall for Herschel-Bulkley and Bingham fluids.

1.1 Nomenclature

m	the number of radial increments in the numerical mesh network
p	the pressure
t	the fluid temperature at any point
t_0	the fluid temperature at annulus entry
t_w	the isothermal wall temperature
p_0	the initial pressure
P	the dimensionless pressure
r, θ and z	the cylindrical coordinates
R, Z	the dimensionless coordinates in the radial and axial directions, respectively
R_1, R_2	the radius of the inner and outer cylinders, respectively
B	the Bingham number
Re, T_a	the modified Reynolds number and Taylor number respectively
N	the aspect ratio of the annulus
$u, v,$ and w	the velocity components in z, r, θ directions, respectively
u_0	the uniform inlet velocity
U, V, W	the dimensionless velocity components
ρ	the density of the fluid
μ	the viscosity of the fluid
μ_r	the reference viscosity

ω	the regular angular velocity
$\Delta R, \Delta Z$	the mesh sizes in the radial and axial directions, respectively.

In the present work, the problem of entrance region flow heat transfer of Bingham fluid in concentric annuli has been investigated. The analysis has been carried out under the assumption that the inner cylinder is rotating and the outer cylinder is at rest. With Prandtl's boundary layer assumptions, the equations of conservation of mass, momentum and energy are discretized and solved using linearized implicit finite difference technique. The system of linear algebraic equations thus obtained has been solved by the Gauss-Jordan method. The development of axial velocity profile, radial velocity profile, tangential velocity profile, pressure drop and the temperature distribution in the entrance region have been determined for different values of non-Newtonian flow characteristics and geometrical parameters. The effects of these on the temperature distribution have been discussed.

2 Formulation of the problem

The geometry of the problem is shown in Fig. 1. The Bingham fluid enters the horizontal concentric annuli with inner and outer radii R_1 and R_2 , respectively, from a large chamber with a uniform flat velocity profile u_0 along the axial direction z and with an initial pressure p_0 and temperature t_0 . The inner cylinder rotates with an angular velocity ω and the outer cylinder is at rest. The flow is steady, laminar, incompressible, axisymmetric with constant physical properties, having negligible viscous dissipation and no internal heat generation. Moreover, it is assumed that the axial heat diffusion is negligible as compared to the radial diffusion. We consider a cylindrical polar coordinate system with the origin at the inlet section on the central axis of the annulus, the z -axis along the axial direction and the radial direction r perpendicular to the z -axis.

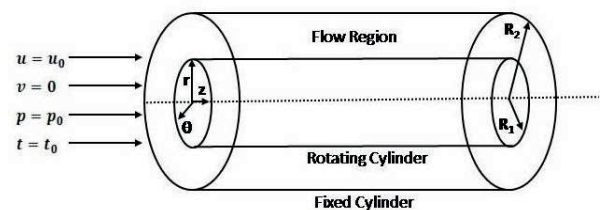


Fig. 1 Geometry of the Problem

Under the above assumptions with the usual Prandtl's boundary layer assumptions [14], the governing equations in polar coordinate system (r, θ, z) for a Bingham fluid in the entrance region are:

$$\text{Continuity equation: } \frac{\partial(rv)}{\partial r} + \frac{\partial(ru)}{\partial z} = 0 \quad (2)$$

$$r - \text{momentum equation: } \frac{w^2}{r} = \frac{1}{\rho} \frac{\partial p}{\partial r} \quad (3)$$

θ - momentum equation :

$$v \frac{\partial w}{\partial r} + u \frac{\partial w}{\partial z} + \frac{vw}{r} = \frac{1}{\rho r^2} \frac{\partial}{\partial r} \left(r^2 \left[\tau_0 + \mu r \frac{\partial}{\partial r} \left(\frac{w}{r} \right) \right] \right) \quad (4)$$

z - momentum equation :

$$v \frac{\partial u}{\partial r} + u \frac{\partial u}{\partial z} = -\frac{1}{\rho} \frac{\partial p}{\partial z} + \frac{1}{\rho r} \frac{\partial}{\partial r} \left(r \left[\tau_0 + \mu \frac{\partial u}{\partial r} \right] \right) \quad (5)$$

$$\text{Energy equation: } v \frac{\partial t}{\partial r} + u \frac{\partial t}{\partial z} = \alpha \left[\frac{\partial^2 t}{\partial r^2} + \frac{1}{r} \frac{\partial t}{\partial r} \right] \quad (6)$$

where u , v , w are the velocity components in z , r , θ directions respectively, t is fluid temperature at any point, ρ is the density of the fluid, α is the thermal diffusivity and p is the pressure.

The boundary conditions associated with the hydrodynamic part of the problem are given by

$$\begin{aligned} \text{for } z \geq 0 \text{ and } r = R_1, v = u = 0 \text{ and } w = \omega R_1 \\ \text{for } z \geq 0 \text{ and } r = R_2, v = u = w = 0 \\ \text{for } z = 0 \text{ and } R_1 < r < R_2, u = u_0 \\ \text{at } z = 0, p = p_0 \end{aligned} \quad (7)$$

Using the boundary conditions (7), the continuity Eq. (2) can be expressed in the following integral form:

$$2 \int_{R_1}^{R_2} r u dr = (R_2^2 - R_1^2) u_0 \quad (8)$$

Introducing the following dimensionless variables and parameters,

$$\begin{aligned} R = \frac{r}{R_2}, U = \frac{u}{u_0}, V = \frac{\rho v R_2}{\mu_r}, W = \frac{w}{\omega R_1}, N = \frac{R_1}{R_2}, \\ P = \frac{p - p_0}{\rho u_0^2}, Z = \frac{2z(1-N)}{R_2 Re}, T = \frac{t - t_0}{t_w - t_0} \\ B = \frac{\tau_0 R_2}{\mu u_0}, T_a = \frac{2\omega^2 \rho^2 R_1^2 (R_2 - R_1)^3}{\mu_r^2 (R_1 + R_2)}, \\ \mu_r = \mu \left(\frac{\omega R_1}{R_2} \right), Re = \frac{2\rho (R_2 - R_1) u_0}{k}, Pr = \frac{\mu C_p}{K} \end{aligned}$$

Here B is the Bingham number, Re Reynolds number, T_a Taylors number, μ_r is know as reference viscosity, Pr is the Prandtl's number, C_p is the specific heat at constant temperature, K is the thermal conductivity and N is known as aspect ratio of the annulus.

Equations (2)-(6) and (8) in the dimensionless form are given by

$$\frac{\partial V}{\partial R} + \frac{V}{R} + \frac{\partial U}{\partial Z} = 0 \quad (9)$$

$$\frac{W^2}{R} = \frac{Re^2 (1-N)}{2(1+N) T_a} \frac{\partial P}{\partial R} \quad (10)$$

$$V \frac{\partial W}{\partial R} + U \frac{\partial W}{\partial Z} + \frac{VW}{R} = \frac{\partial^2 W}{\partial R^2} + \frac{1}{R} \frac{\partial W}{\partial R} - \frac{W}{R^2} + \frac{2B}{R} \quad (11)$$

$$V \frac{\partial U}{\partial R} + U \frac{\partial U}{\partial Z} = -\frac{\partial P}{\partial Z} + \frac{1}{R} \frac{\partial U}{\partial R} + \frac{\partial^2 U}{\partial R^2} + \frac{B}{R} \quad (12)$$

$$V \frac{\partial T}{\partial R} + U \frac{\partial T}{\partial Z} = \frac{1}{Pr} \left[\frac{\partial^2 T}{\partial R^2} + \frac{1}{R} \frac{\partial T}{\partial R} \right] \quad (13)$$

and

$$2 \int_N^1 R U dR = (1 - N^2) \quad (14)$$

The boundary conditions (7) associated with the hydrodynamic part of the problem in the dimensionless form are given by

$$\begin{aligned} \text{for } Z \geq 0 \text{ and } R = N, V = U = 0 \text{ and } W = 1 \\ \text{for } Z \geq 0 \text{ and } R = 1, V = U = W = 0 \\ \text{for } Z = 0 \text{ and } N < R < 1, U = 1 \\ \text{at } Z = 0, P = 0 \end{aligned} \quad (15)$$

For the thermal part, considering the outer cylinder to be adiabatic and the inner cylinder to be isothermal, the problem has been solved under the following boundary conditions:

$$\begin{aligned} \text{for } Z \geq 0, T = 1 \text{ at } R = N \\ \text{for } Z \geq 0, \frac{\partial T}{\partial R} = 0 \text{ at } R = 1 \\ \text{for } Z = 0 \text{ and } N < R < 1, T = 0 \end{aligned} \quad (16)$$

The problem can be similarly analyzed for the case when the inner cylinder is adiabatic and the outer cylinder is isothermal. The boundary conditions for this case will be

$$\begin{aligned} \text{for } Z \geq 0, T = 1 \text{ at } R = 1 \\ \text{for } Z \geq 0, \frac{\partial T}{\partial R} = 0 \text{ at } R = N \\ \text{for } Z = 0 \text{ and } N < R < 1, T = 0 \end{aligned} \quad (17)$$

3 Numerical solution

The numerical analysis and the method of solution adopted here can be considered as an indirect extension of the work of Coney and El-Shaarawi [1]. Considering the mesh network of Fig. 2, the following difference representations are made. Here ΔR and ΔZ represent the grid size along the radial and axial directions respectively.

$$V_{i+1,j+1} = V_{i,j+1} \left(\frac{N + i\Delta R}{N + (i+1)\Delta R} \right) - \frac{\Delta R}{4\Delta Z} \left(\frac{2N + (2i+1)\Delta R}{N + (i+1)\Delta R} \right) (U_{i+1,j+1} + U_{i,j+1} - U_{i+1,j} - U_{i,j}) \quad (18)$$

$$\frac{W_{i,j+1}^2}{N + i\Delta R} = \frac{(1-N)Re^2}{2T_a(1+N)} \frac{P_{i,j+1} - P_{i-1,j+1}}{\Delta R} \quad (19)$$

$$Vi, j \left[\frac{W_{i+1,j+1} + W_{i+1,j} - W_{i-1,j} - W_{i-1,j+1}}{4\Delta R} \right] + Ui, j \left[\frac{W_{i,j+1} - W_{i,j}}{\Delta Z} \right] + \frac{V_{i,j}W_{i,j}}{N + i\Delta R} = \frac{W_{i+1,j+1} + W_{i+1,j} - 2W_{i,j+1} - 2W_{i,j} + W_{i-1,j} + W_{i-1,j+1}}{2(\Delta R)^2} + \frac{W_{i+1,j+1} + W_{i+1,j} - W_{i-1,j} - W_{i-1,j+1}}{(N + i\Delta R)4\Delta R} - \frac{W_{ij}}{(N + i\Delta R)^2} + \frac{2B}{N + i\Delta R} \quad (20)$$

$$Vi, j \left[\frac{U_{i+1,j+1} - U_{i-1,j+1}}{2\Delta R} \right] + Ui, j \left[\frac{U_{i,j+1} - U_{i,j}}{\Delta Z} \right] = - \left[\frac{P_{i,j+1} - P_{i,j}}{\Delta Z} \right] + \left[\frac{U_{i+1,j+1} - U_{i-1,j+1}}{(N + i\Delta R)2\Delta R} \right] + \left[\frac{U_{i+1,j+1} - 2U_{i,j+1} + U_{i-1,j+1}}{(\Delta R)^2} \right] + \frac{B}{N + i\Delta R} \quad (21)$$

where $i = 0$ at $R = N$ and $i = m$ at $R = 1$.

The application of trapezoidal rule to Eq. (14) gives

$$\frac{\Delta R}{2} (NU_{0,j} + U_{m,j}) + \Delta R \sum_{i=1}^{m-1} U_{i,j} (N + i\Delta R) = \left(\frac{1 - N^2}{2} \right)$$

The boundary condition (15) gives $U_{0,j} = U_{m,j} = 0$ and the above equation reduces to

$$\Delta R \sum_{i=1}^{m-1} U_{i,j} (N + i\Delta R) = \left(\frac{1 - N^2}{2} \right) \quad (22)$$

The set of difference Eqs. (18)-(22) have been solved by the iterative procedure. Starting at the $j = 0$ column (annulus entrance) and applying Eq. (20) for $1 \leq i \leq m - 1$, we get a system of linear algebraic equations. This system has been solved by using Gauss-Jordan method to obtain the values of the

velocity component W at the second column $j = 1$. Then applying Eqs. (19) and (21) for $1 \leq i \leq m - 1$ and Eq. (22), we get a system of linear equations. Again solving this system by Gauss-Jordan method to obtain the values of the velocity component U and the pressure P at the second column $j = 1$. Finally, the values of the velocity component V at the second column $j = 1$ are obtained from Eq. (18) by Gauss-Jordan method using the known values of U . Repeating this procedure, we can advance, column by column, along the axial direction of the annulus until the flow becomes axially and tangentially fully developed.

With the values of V and U known, the energy Eq. (13) can be considered as a linear equation in T with variable coefficients. By using the implicit finite difference technique, the energy equation can be represented as

$$Ti+1, j+1 \left[\frac{V_{i,j+1} + V_{i,j}}{8\Delta R} - \frac{1}{2Pr(\Delta R)^2} - \frac{1}{4(N + i\Delta R)Pr\Delta R} \right] + Ti, j+1 \left[\frac{U_{i,j+1} + U_{i,j}}{2\Delta Z} + \frac{1}{Pr(\Delta R)^2} \right] + Ti-1, j+1 \left[\frac{1}{4(N + i\Delta R)Pr\Delta R} - \frac{V_{i,j+1} + V_{i,j}}{8\Delta R} - \frac{1}{2Pr(\Delta R)^2} \right] = Ti, j \left[\frac{U_{i,j+1} + U_{i,j}}{2\Delta Z} - \frac{1}{Pr(\Delta R)^2} \right] + Ti+1, j \left[\frac{1}{2Pr(\Delta R)^2} + \frac{1}{4(N + i\Delta R)Pr\Delta R} - \frac{V_{i,j+1} + V_{i,j}}{8\Delta R} \right] + Ti-1, j \left[\frac{V_{i,j+1} + V_{i,j}}{8\Delta R} + \frac{1}{2Pr(\Delta R)^2} - \frac{1}{4(N + i\Delta R)Pr\Delta R} \right] \quad (23)$$

Equation (23), with the boundary conditions (16), have been solved to obtain the temperature profiles in the annular entrance region. The system of linear equations associated with each column has been solved by Gauss-Jordan elimination method.

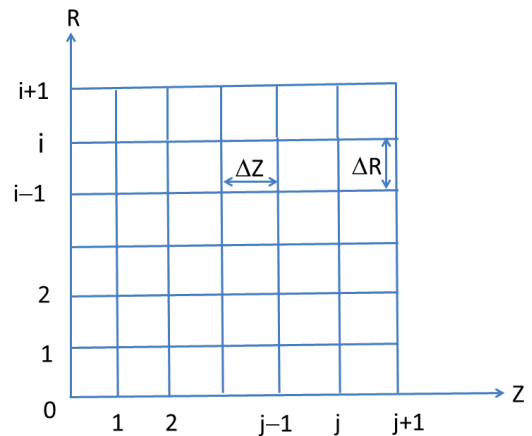


Fig. 2 Grid Formation for Finite-Difference Representations

4 Results and Discussion

Numerical calculations have been performed for all admissible values of Bingham number B and aspect ratio N . The Prandtl's number has been chosen initially as 7 and gradually increased to 15. The ratio of Reynolds number to Taylor number $Rt = Re^2 / T_a = 20, 10, \Delta Z = 0.02, 0.03$ and $\Delta R = 0.1, 0.05$ have been fixed for $N = 0.3$ and 0.8 respectively. The velocity profiles, pressure drop and temperature distribution along radial direction

have been computed for $N = 0.3, 0.8$ and $B = 0, 10, 20, 30$. The temperature distribution along radial direction have been plotted for different axial positions with $N = 0.3, 0.8, B = 0, 10, 20, 30$ and $Pr = 7, 10$ and 15. The effects of non-Newtonian characteristics and geometrical parameters on velocity profiles and pressure drop have been extensively discussed elsewhere [13]. Here the temperature distributions during the rotation of the inner wall of the annuli have been shown in Figs. 3-26.

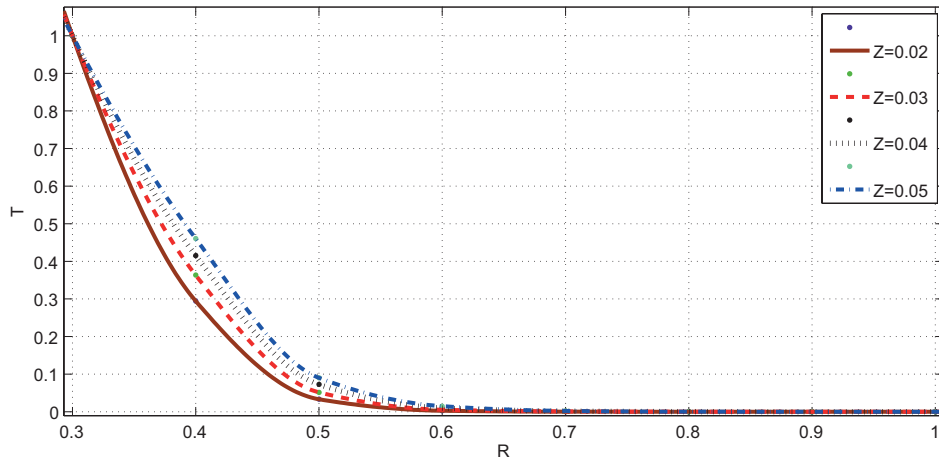


Fig. 3 Temperature Distribution for $N = 0.3, Pr = 7$ and $B = 0$

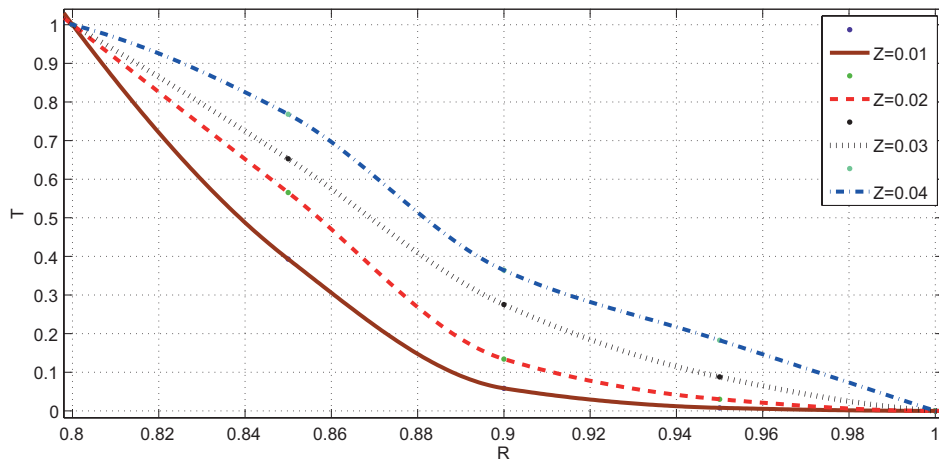


Fig. 4 Temperature Distribution for $N = 0.8, Pr = 7$ and $B = 0$

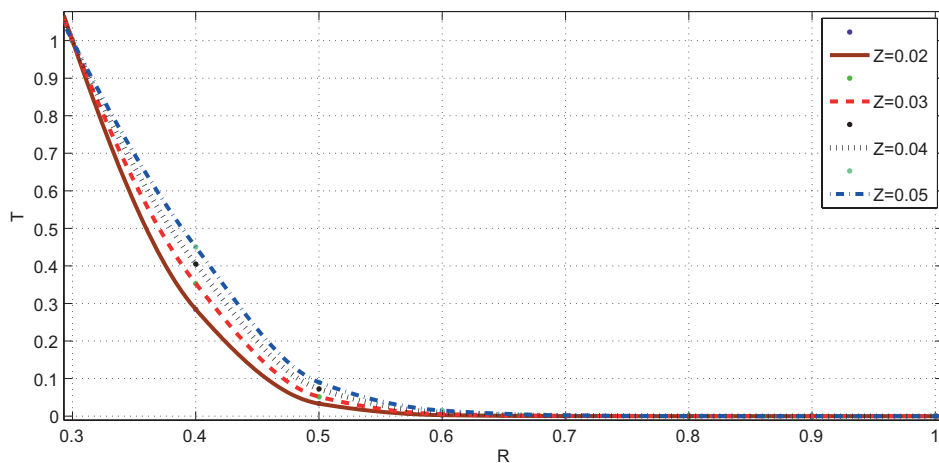


Fig. 5 Temperature Distribution for $N = 0.3, Pr = 7$ and $B = 10$

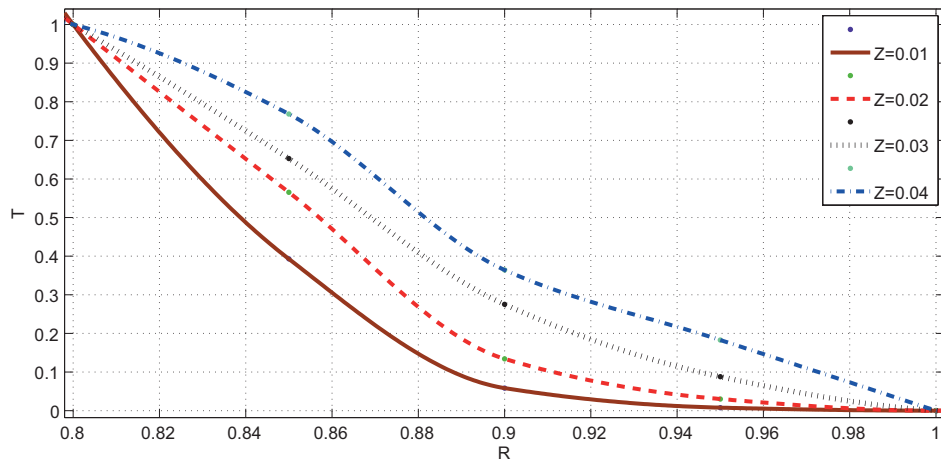


Fig. 6 Temperature Distribution for $N=0.8$, $Pr=7$ and $B=10$

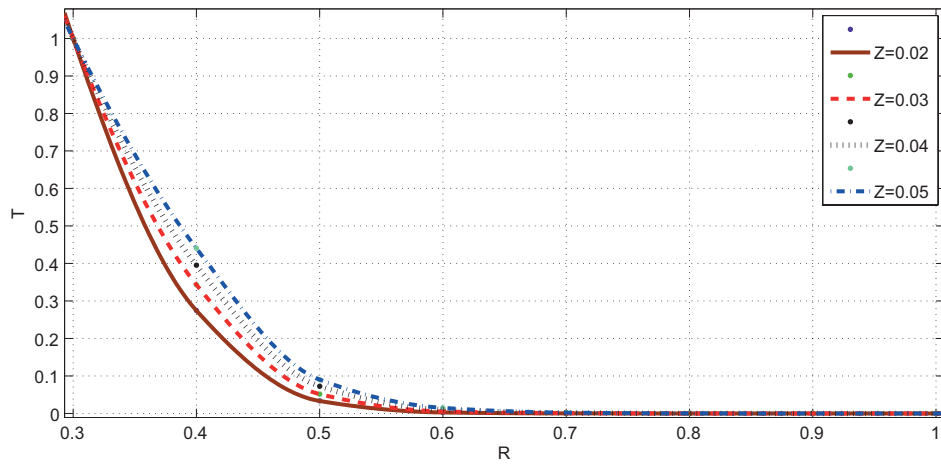


Fig. 7 Temperature Distribution for $N=0.3$, $Pr=7$ and $B=20$

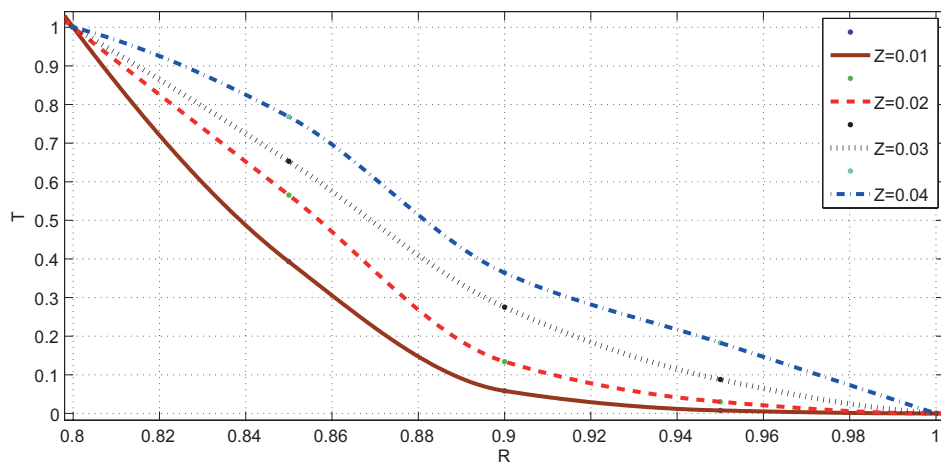


Fig. 8 Temperature Distribution for $N=0.8$, $Pr=7$ and $B=20$

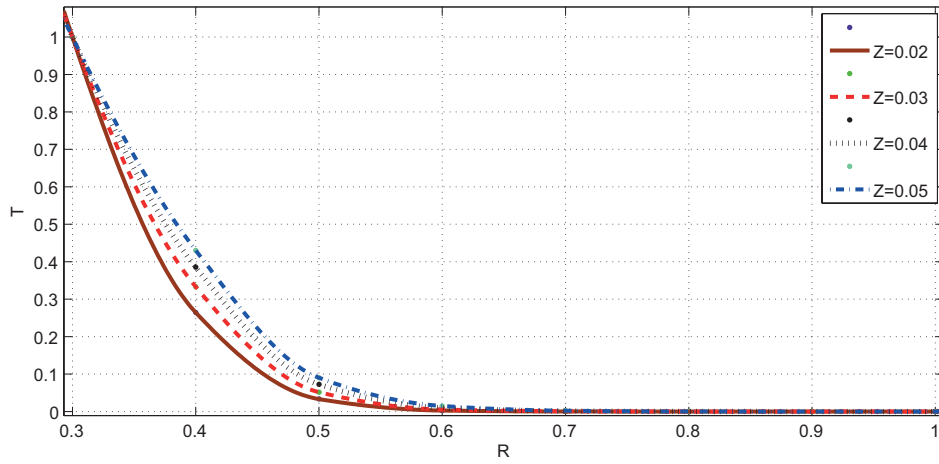


Fig. 9 Temperature Distribution for $N = 0.3$, $Pr = 7$ and $B = 30$

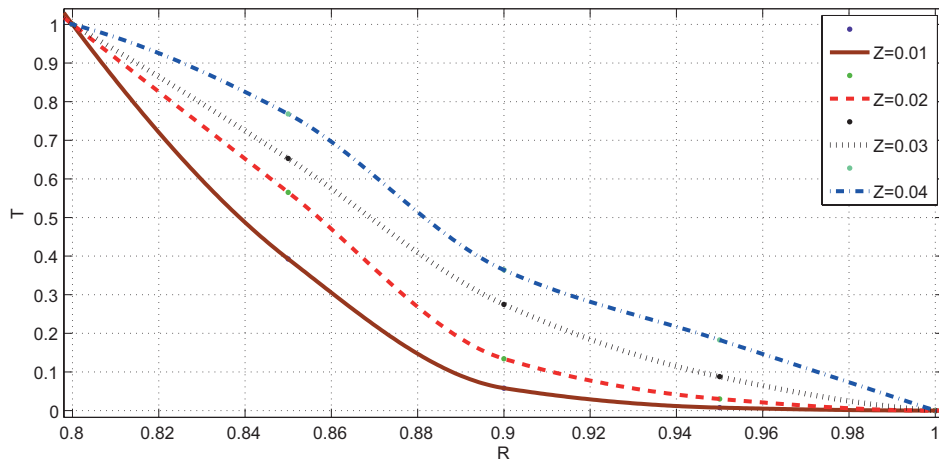


Fig. 10 Temperature Distribution for $N = 0.8$, $Pr = 7$ and $B = 30$

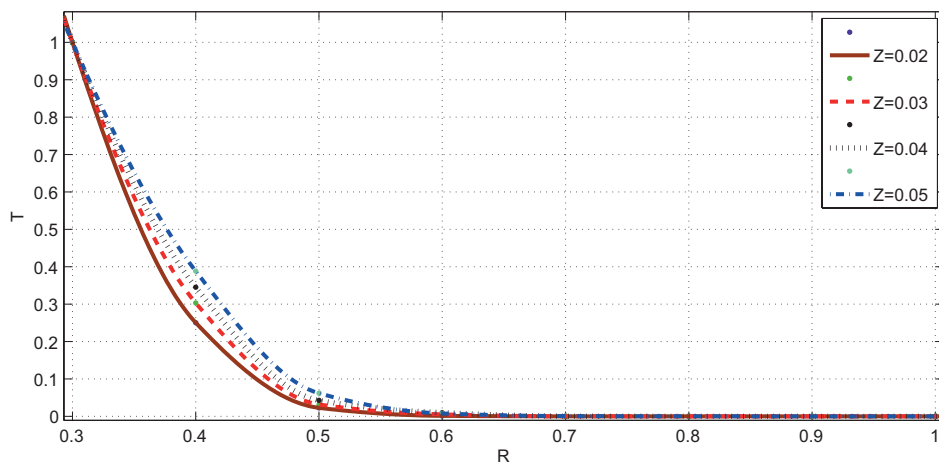


Fig. 11 Temperature Distribution for $N = 0.3$, $Pr = 10$ and $B = 0$

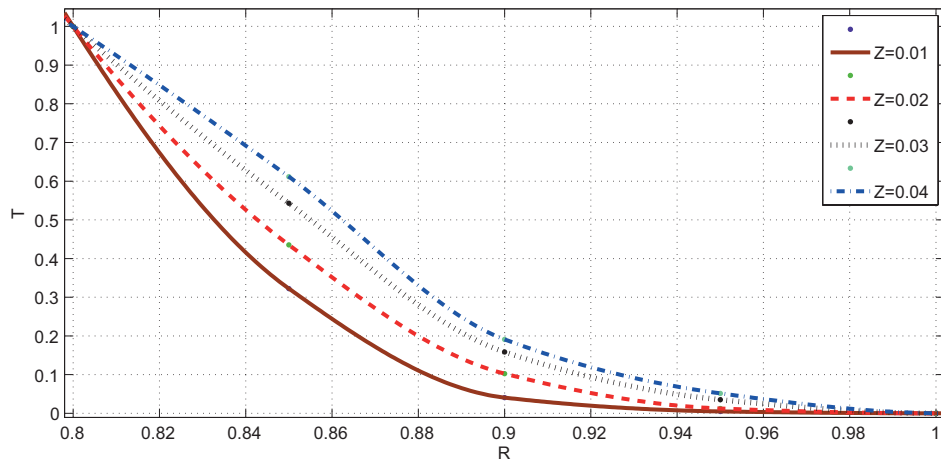


Fig. 12 Temperature Distribution for $N = 0.8$, $Pr = 10$ and $B = 0$

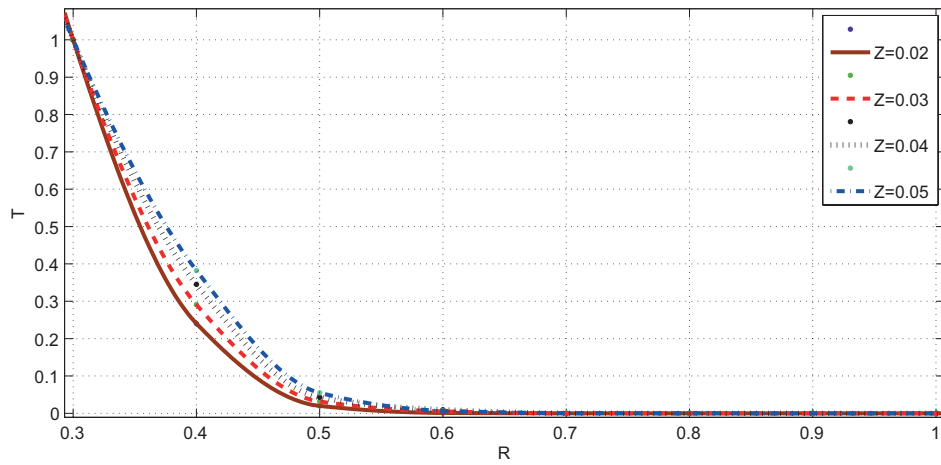


Fig. 13 Temperature Distribution for $N = 0.3$, $Pr = 10$ and $B = 10$

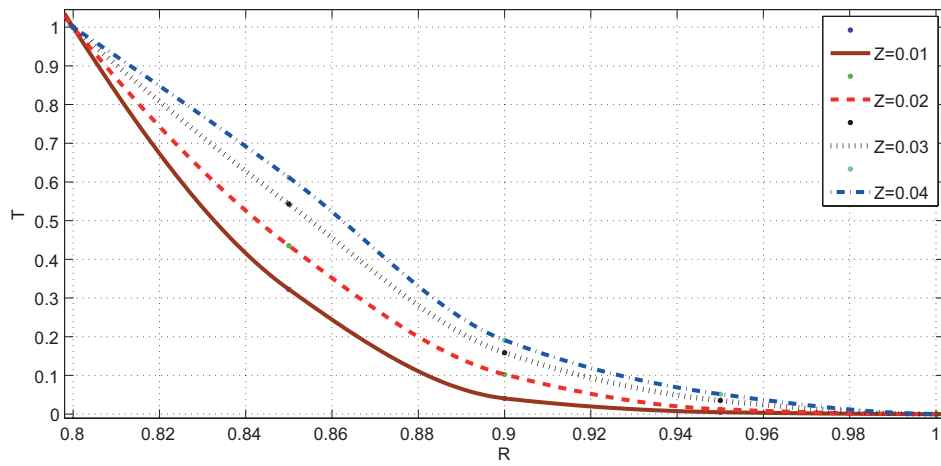


Fig. 14 Temperature Distribution for $N = 0.8$, $Pr = 10$ and $B = 10$

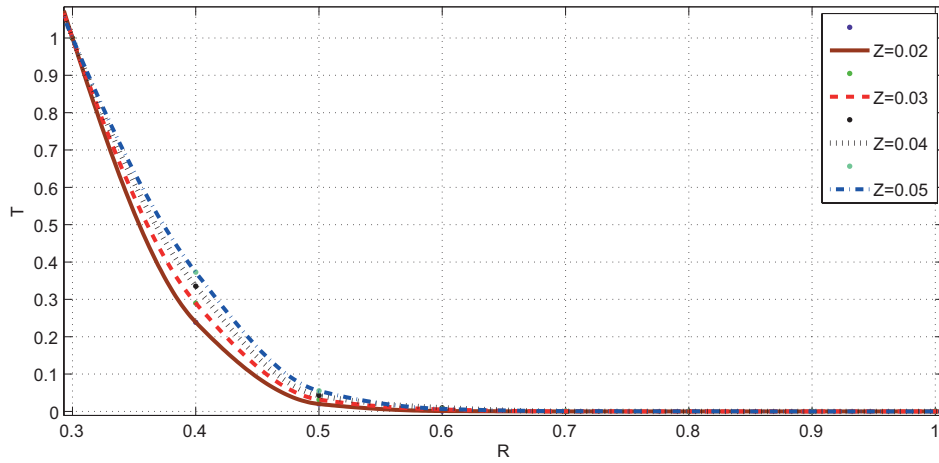


Fig. 15 Temperature Distribution for $N = 0.3$, $Pr = 10$ and $B = 20$

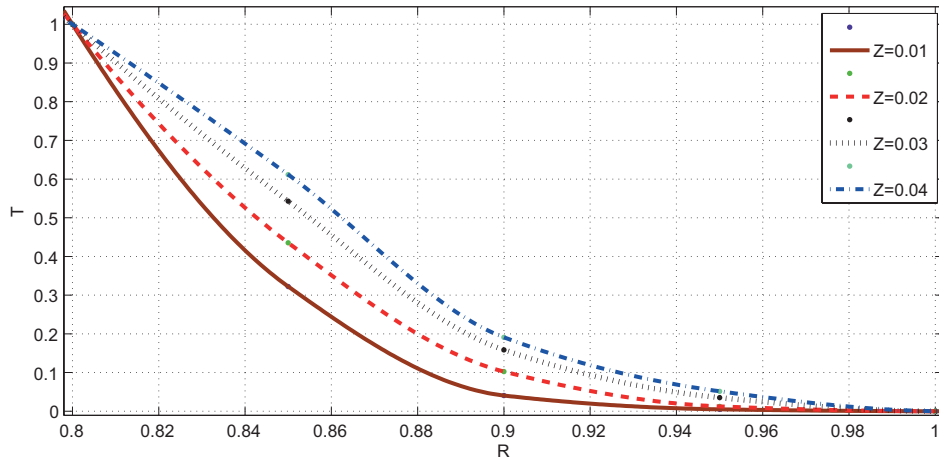


Fig. 16 Temperature Distribution for $N = 0.8$, $Pr = 10$ and $B = 20$

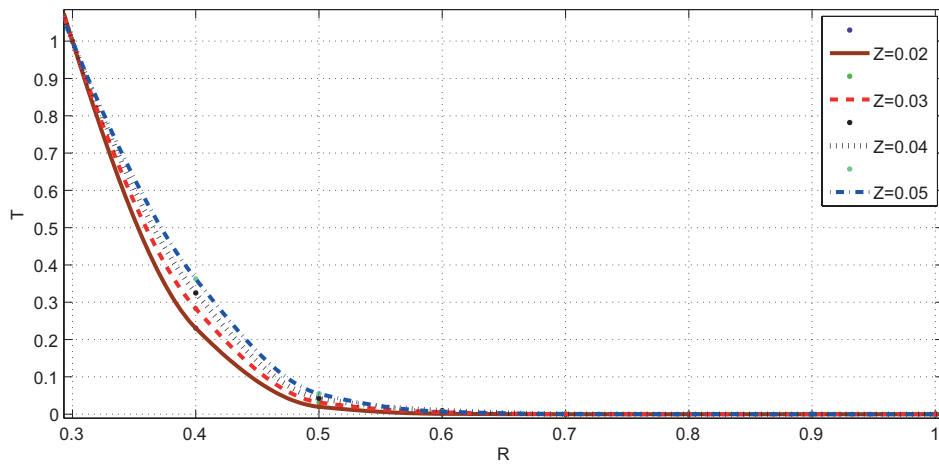


Fig. 17 Temperature Distribution for $N = 0.3$, $Pr = 10$ and $B = 30$

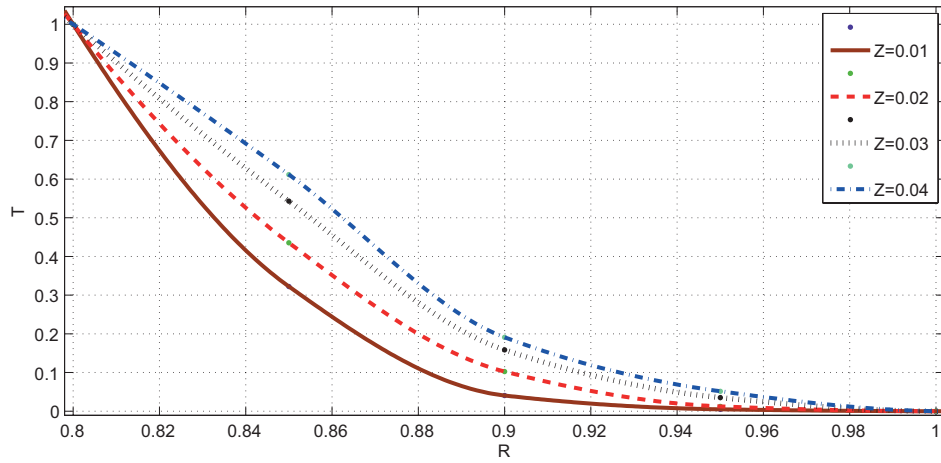


Fig. 18 Temperature Distribution for $N=0.8$, $Pr=10$ and $B=30$

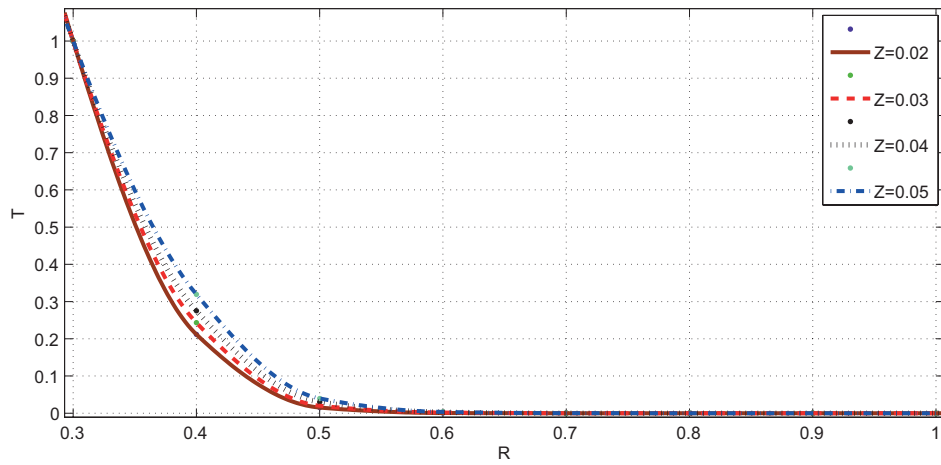


Fig. 19 Temperature Distribution for $N=0.3$, $Pr=15$ and $B=0$

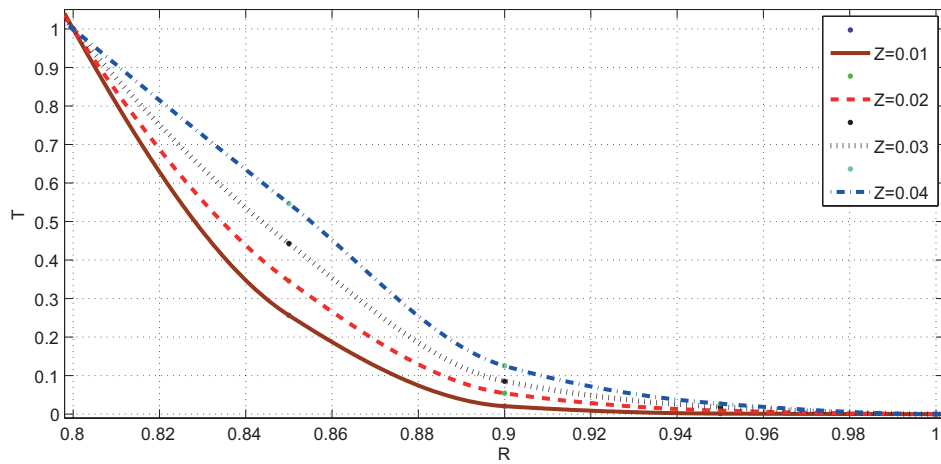


Fig. 20 Temperature Distribution for $N=0.8$, $Pr=15$ and $B=0$

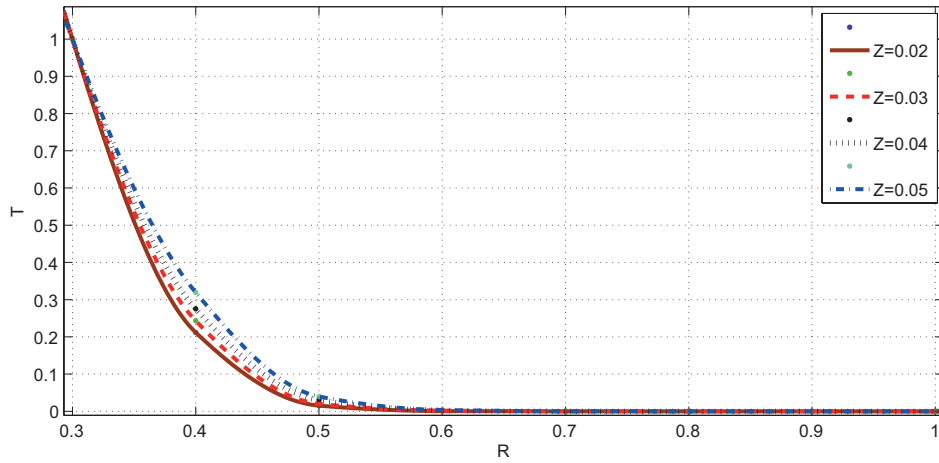


Fig. 21 Temperature Distribution for $N = 0.3$, $Pr = 15$ and $B = 10$

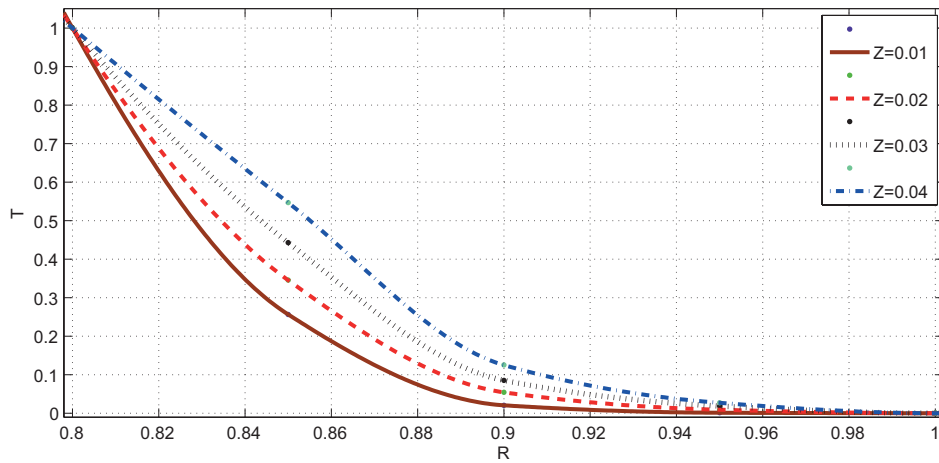


Fig. 22 Temperature Distribution for $N = 0.8$, $Pr = 15$ and $B = 10$

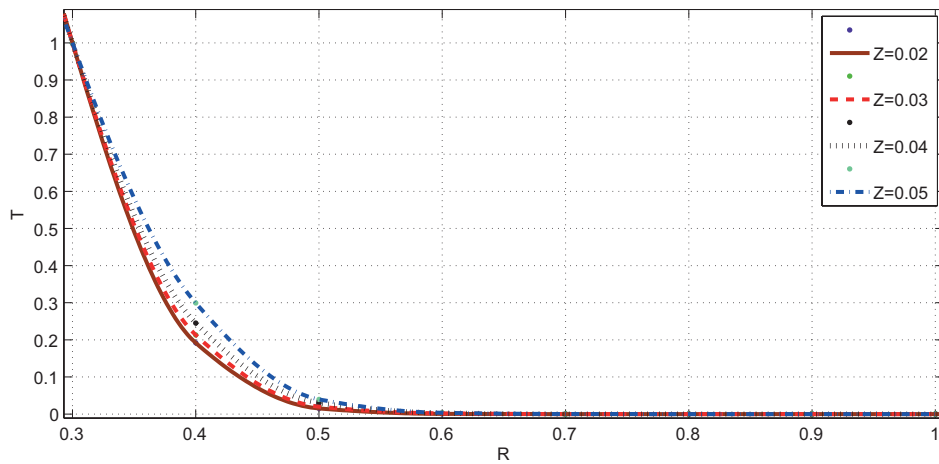


Fig. 23 Temperature Distribution for $N = 0.3$, $Pr = 15$ and $B = 20$

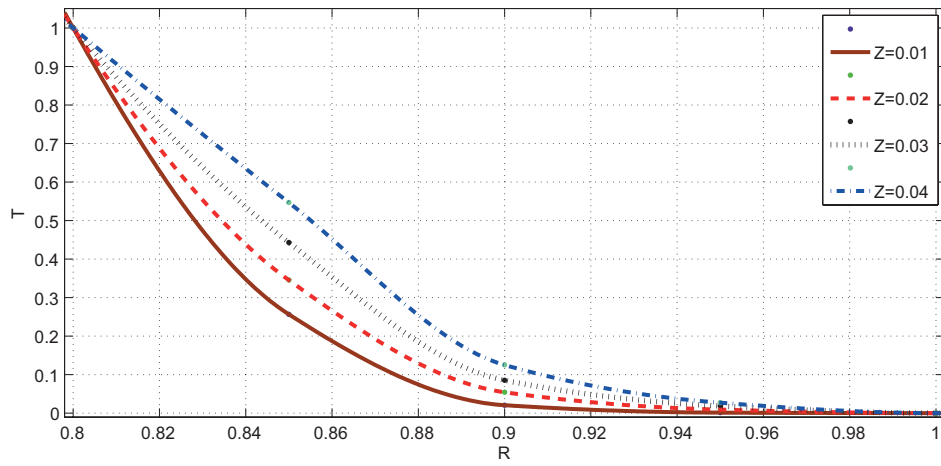


Fig. 24 Temperature Distribution for $N=0.8$, $Pr=15$ and $B=20$

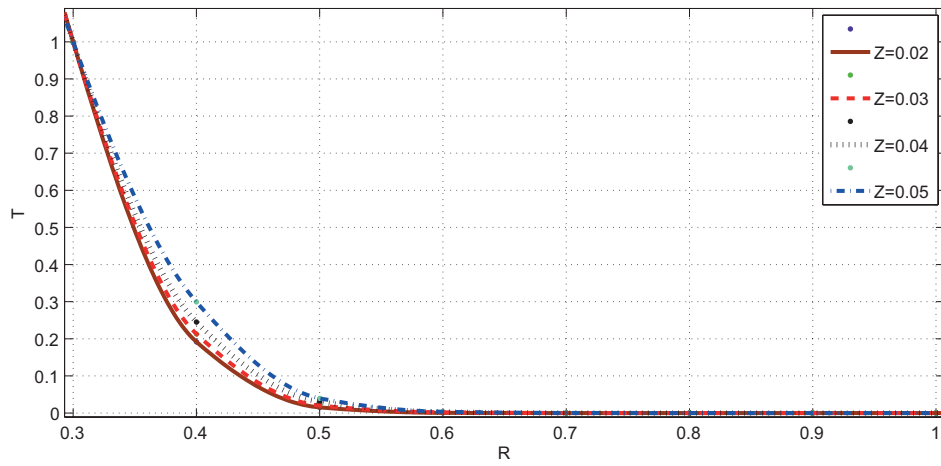


Fig. 25 Temperature Distribution for $N=0.3$, $Pr=15$ and $B=30$

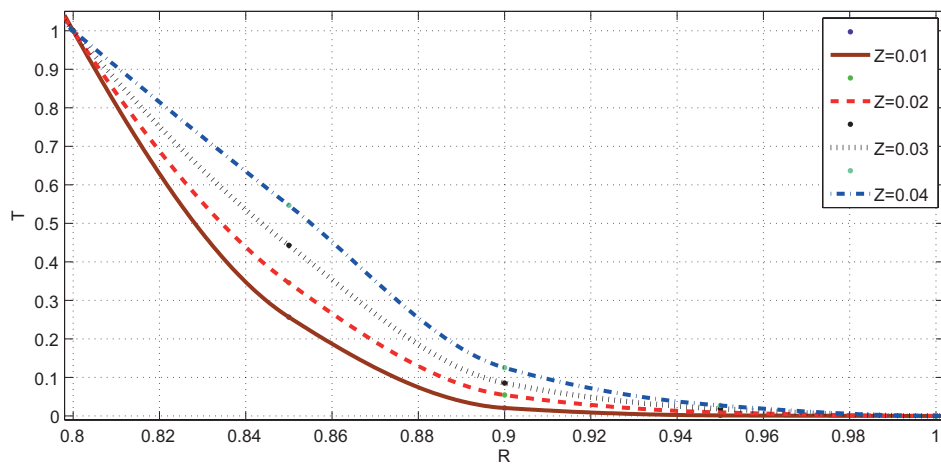


Fig. 26 Temperature Distribution for $N=0.8$, $Pr=15$ and $B=30$

It is observed from the results obtained, that the temperature decreases with increase of Bingham number B for a fixed annular width. When the aspect ratio N increases, it is found that the temperature increases for a fixed Bingham number.

Moreover, with the increase of Prandtl's numbers the temperature decreases for a fixed aspect ratio N and Bingham number B . Also, it is found that with the increase of axial position the temperature also increasing for a fixed aspect ratio N , Bingham number B and Prandtl's number.

The present results are compared with available results in literature for various particular cases and are found to be in agreement. When the Bingham number $B = 0$, our results match with the results corresponded to Newtonian fluid of Coney and El-Shaarawi [1]. In the case of stationary cylinders, the results in our analysis are matching with the results of Kandasamy [7]. Also, in the case of non-thermal part these results matches with the results of Srinivasa Rao and Kandasamy [13].

5 Conclusions

Numerical results for the entrance region flow heat transfer in concentric annuli with rotating inner wall for Bingham fluid were presented. The effects of the parameters aspect ratio N , Bingham number B and Prandtl's number on the temperature distribution are studied. Numerical calculations have been performed for all admissible values of aspect ratio N , Bingham number B and Prandtl's number. The temperature distribution along radial direction R have been presented geometrically. The present results are found in agreement with the results corresponding to various particular cases available in literature.

From this study, the following can be concluded.

1. The temperature decreases from the rotating inner wall to the stationary outer wall of the annulus.
2. When increasing the Bingham numbers B , it is observed that the temperature decreases.
3. With the increase of Prandtl's numbers, the temperature decreases.
4. When aspect ratio N increases, it is found that the temperature increases.
5. With the increase of axial position Z , the temperature also increases.

References

- [1] Coney, J. E. R., El-Shaarawi, M. A. I. "A contribution to the numerical solution of developing laminar flow in the entrance region of concentric annuli with rotating inner walls." *Journal of Fluids Engineering*. 96(4), pp. 333-340. 1974. DOI: [10.1115/1.3447166](https://doi.org/10.1115/1.3447166)
- [2] Mishra, I. M., Kumar, S., Mishra, P. "Entrance Region Flow of Bingham Plastic Fluids in Concentric Annulus." *Indian Journal of Technology*. 23, pp. 81-87. 1985.
- [3] Batra, R. L., Das, B. "Flow of a Casson Fluid between Two Rotating Cylinders." *Fluid Dynamic Research*. 9, pp. 133-141. 1992. DOI: [10.1016/0169-5983\(92\)90063-3](https://doi.org/10.1016/0169-5983(92)90063-3)
- [4] Maia, M. C. A., Gasparetto, C. A. "A numerical solution for entrance region of non-Newtonian flow in annuli." *Brazilian Journal of Chemical Engineering*. 20(2), pp. 201-211. 2003. DOI: [10.1590/s0104-66322003000200014](https://doi.org/10.1590/s0104-66322003000200014)
- [5] Sayed-Ahmed, M. E., Sharaf-El-Din, H. "Entrance region flow of a power-law fluid in concentric annuli with rotating inner wall." *International Communications in Heat and Mass Transfer*. 33(5), pp. 654-665. 2006. DOI: [10.1016/j.icheatmasstransfer.2006.01.004](https://doi.org/10.1016/j.icheatmasstransfer.2006.01.004)
- [6] Bird, R. D., Dai, G. C., Yarusso, B. J. "The rheology and flow of viscoplastic materials." *Reviews in Chemical Engineering*. 1, pp. 1-70. 1982.
- [7] Kandasamy, A. "Entrance region flow heat transfer in concentric annuli for a Bingham fluid." In: Third Asian-Pacific Conference on Computational Mechanics, Seoul, Korea, Sept. 16-18, 1996. pp. 1697-1702.
- [8] Round, G. F., Yu, S. "Entrance laminar flows of viscoplastic fluids in concentric annuli." *The Canadian Journal of Chemical Engineering*. 71(4), pp. 642-645. 1993. DOI: [10.1002/cjce.5450710417](https://doi.org/10.1002/cjce.5450710417)
- [9] Galanis, N., Rashidi, M. M. "Entropy generation in Non-Newtonian fluids due to heat and mass transfer in the entrance region of ducts." *Heat and Mass Transfer*. 48(9), pp. 1647-1662. 2012. DOI: [10.1007/s00231-012-1009-7](https://doi.org/10.1007/s00231-012-1009-7)
- [10] Rashidi, M. M., Keimanesh, M., Rajvanshi, S. C., Wasu, S. "Pulsatile flow through annular space bounded by outer porous cylinder and an inner cylinder of permeable material." *International Journal for Computational Methods in Engineering Science and Mechanics*. 13(6), pp. 381-391. 2012. DOI: [10.1080/15502287.2012.698708](https://doi.org/10.1080/15502287.2012.698708)
- [11] Rashidi, M. M., Rajvanshi, S. C., Kavyani, N., Keimanesh, M., Pop, I., Saini, B. S. "Investigation of Heat Transfer in a Porous Annulus with Pulsating Pressure Gradient by Homotopy Analysis Method." *Arabian Journal for Science and Engineering*. 39(6), pp. 5113-5128. 2014. DOI: [10.1007/s13369-014-1140-5](https://doi.org/10.1007/s13369-014-1140-5)
- [12] Kandasamy, A., Nadiminti, S. R. "Entrance region flow in concentric annuli with rotating inner wall for Herschel-Bulkley fluids." *International Journal of Applied and Computational Mathematics*. 1(2), pp. 235-249. 2015. DOI: [10.1007/s40819-015-0029-7](https://doi.org/10.1007/s40819-015-0029-7)
- [13] Nadiminti, S. R., Kandasamy, A. "Entrance region flow in concentric annuli with rotating inner wall for Bingham fluid." In: Proceedings of the 16th International Conference on Fluid Flow Technology (CMFF'15), Budapest, Hungary, Sept. 1-4, 2015.
- [14] Schlichting H., Gersten, K. "Boundary Layer Theory." 8th ed., Springer, 2000.